



Elucidating various geochemical mechanisms drive fluoride contamination in unconfined aquifers along the major rivers in Sindh and Punjab, Pakistan[☆]

Waqar Ali^{a, b}, Muhammad Wajahat Aslam^{a, b}, Muhammad Junaid^c, Kamran Ali^d, Yongkun Guo^{a, e}, Atta Rasool^{a, b}, Hua Zhang^{a, *}

^a State Key Laboratory of Environmental Geochemistry, Institute of Geochemistry, Chinese Academy of Sciences, Guiyang, 550081, China

^b University of Chinese Academy of Sciences, Beijing, 100049, China

^c Key Laboratory for Heavy Metal Pollution Control and Reutilization, School of Environment and Energy, Peking University Shenzhen Graduate School, Shenzhen, 518055, China

^d Institute of Environmental Sciences and Engineering (IESE), School of Civil and Environmental Engineering (SCEE), National University of Science and Technology (NUST), Islamabad, Pakistan

^e Collage of Life Science, Sichuan Normal University, China

ARTICLE INFO

Article history:

Received 22 December 2018

Received in revised form

10 March 2019

Accepted 11 March 2019

Available online 21 March 2019

Keywords:

Fluoride

Groundwater

Mechanisms

Unconfined aquifer

Pakistan

ABSTRACT

The present study aims to investigate the spatial distribution and associated various geochemical mechanisms responsible for fluoride (F⁻) contamination in groundwater of unconfined aquifer system along major rivers in Sindh and Punjab, Pakistan. The concentration of F⁻ in groundwater samples ranged from 0.1 to 3.9 mg/L (mean = 1.0 mg/L) in Sindh and 0.1–10.3 mg/L (mean = 1.0 mg/L) in Punjab, respectively with 28.9% and 26.6% of samples exhibited F⁻ contamination beyond WHO permissible limit value (1.5 mg/L). The geochemical processes regulated F⁻ concentration in unconfined aquifer mainly in Sindh and Punjab were categorized as follows: 1) minerals weathering that observed as the key process to control groundwater chemistry in the study areas, 2) the strong correlation between F⁻ and alkaline pH, which provided favorable environmental conditions to promote F⁻ leaching through desorption or by ion exchange process, 3) the 72.6% of samples from Sindh and Punjab were dominated by Na⁺-Cl⁻ type of water, confirmed that the halite dissolution process was the major contributor for F⁻ enrichment in groundwater, 4) dolomite dissolution was main process frequently observed in Sindh, compared with Punjab, 5) the arid climatic conditions promote evaporation process or dissolution of evaporites or both were contributing to the formation of saline groundwater in the study area, 6) the positive correlation observed between elevated F⁻ and fluorite also suggested that the fluorite dissolution also played significant role for leaching of F⁻ in groundwater from sediments, and 7) calcite controlled Ca²⁺ level and enhanced the dissolution of F-bearing minerals and drive F⁻ concentration in groundwater. In a nut shell, this study revealed the worst scenarios of F⁻ contamination via various possible geochemical mechanisms in groundwater along major rivers in Sindh and Punjab, Pakistan, which need immediate attention of regulatory authorities to avoid future hazardous implications.

© 2019 Elsevier Ltd. All rights reserved.

1. Introduction

Groundwater is primary source of drinking water worldwide and most of the groundwater resources are severely polluted with

the major ions of toxic trace metals including fluoride (F⁻) (Rashid et al., 2019). These pollutants originated from various natural and anthropogenic sources such as, volcanic activities, weathering and dissolution of mineral deposits, coal incineration, mining activities, surface run off, agricultural activities, steel manufacturing units, surface run off and direct dispose of untreated industrial waste water into riverine system (Jehan et al., 2018; Rashid et al., 2018). Most of toxic ionic pollutants are highly mobile in surface water sources such as rivers, lakes, streams, and natural aquifer system,

[☆] This paper has been recommended for acceptance by Joerg Rinklebe.

* Corresponding author.

E-mail address: zhanghua@mail.gyig.ac.cn (H. Zhang).

bore well, dug well, tube well, natural springs and hand pumps (Ali et al., 2018b; Khan et al., 2016).

The fluorine (F) belongs to halogen family in the periodic table being the lightest member and most electronegative and reactive of all elements (Rafique et al., 2015). Due to its high reactivity, it does not found in elemental form & readily reacts to form inorganic and organic compounds as F⁻ ion (Rasool et al., 2018). It ranked 13th most abundant element covering 0.06–0.09% of the total earth crust (Dehbandi et al., 2017; Rasool et al., 2018). The F⁻ concentration in surface water reported at 0.01–0.3 mg/L, while in groundwater it ranged below 1 mg/L to 35 mg/L (Msonda et al., 2007). Generally, F⁻ can enter the human body mainly by drinking water (Li et al., 2014). The F⁻ < 1.5 mg/L may help to prevent the incidence of dental caries and enhance the growth of bone (Edmunds and Smedley, 2013), however, F⁻ > 1.5 mg/L can cause dental fluorosis or mottled enamel (Rahmani et al., 2010), increased allergic reactions, allergic diseases, fertility effects, and nephrotic effects (KheradPisheh et al., 2016), F⁻ > 3.0 mg/L may cause skeletal fluorosis (Dar et al., 2011; Raj and Shaji, 2017). The previous studies described various mechanisms and geological process including, weathering of minerals dissolution, precipitation, desorption/adsorption, evapotranspiration, ion-exchange, volcanic eruption, complex formation as well as human activities involved in F⁻ enrichment of the groundwater (Brahman et al., 2013; Farooqi et al., 2007; Li et al., 2018; Rasool et al., 2017; Zabala et al., 2016). The previous studies also suggested mixing of numerous water sources such as irrigation return water, saline water, fresh water as well as arid climatic conditions as various driving factors, which facilitated F⁻ enrichment in the groundwater system (Li et al., 2018; Rasool et al., 2017; Rezaei et al., 2017). The Pakistan council for research in water resources (PCRWR) carried out a detailed study and to explore the possibility of F⁻ contamination and associated human health implications such as in the drinking water of sixteen major cities of four provinces and they found F⁻ concentration exceeding the permissible limit 1.5 mg/L (Tahir and Rasheed, 2013). The major sources mainly comprised of phosphate fertilizer, containing leachable F⁻ content at 52.0 to 25.0 mg/kg and coal containing F⁻ content at 5.0–20.0 mg/kg (Ayoob and Gupta, 2006; Farooqi et al., 2007). The children (age <15 year) from Kalalanwala, east Punjab suffered from serious health concerns such as bone deformation, fluorosis and spinal defects (Farooqi et al., 2007). A study was conducted in Nagar Parkar Sindh reported more than 78.0% groundwater samples exceeding F⁻ permissible limit, where 12.5% population exhibited low risk of dental fluorosis, 50.3% population with high dental and mild skeletal fluorosis risks and 12.5% population at very high risk of skeletal fluorosis (Tahir and Rasheed, 2013). Along the riverine system with unconfined aquifer areas of Pakistan, the continuous drawl of groundwater for domestic, agricultural, industrial and drinking purpose is the major cause to deteriorate the quality of groundwater (Podgorski et al., 2017). Furthermore, urbanization, agricultural activities, industrialization, mining activities and waste water discharges along the major riverine systems are the serious environmental concerns in Pakistan (Shahid et al., 2018). The previous studies highlighted elevated F⁻ contamination in groundwater and associated adverse health effects in exposed population of Pakistan (Rasool et al., 2018; Rasool et al., 2015). However, hydrogeochemical mechanisms and key process that drive F⁻ contamination in the groundwater along the riverine systems of the region are still not well defined. Therefore, the main objectives of current study are 1) to monitor the distribution of F⁻ in groundwater samples collected along whole stretch of major riverine system in two provinces, Sindh and Punjab, Pakistan, 2) to categorize the hydro-geochemical processes that control groundwater chemistry, which ultimately affects F⁻ contamination in the study area, and 3) to investigate the key

process responsible for initiation of F⁻ enrichment in unconfined aquifers in the study area.

2. Material and methods

2.1. Geological background of the study area and sample collection

About more than 75 percent population of Pakistan settled in two central provinces of Pakistan, namely, Sindh and Punjab. The study area is mainly categorized as the flat-low-lying Indus plain region (Shahid et al., 2018). It is primarily composed of approximately 300 m of the Quaternary alluvial residues, permeable soils with truncated inorganic content (Ali et al., 2018b; Mushtaq et al., 2018). The climate of this area is semiarid to arid excluding temperate north-west regions (Mushtaq et al., 2018). The unconsolidated gravel and sand deposits of the Quaternary age alluvial are the key factors to development of most aquifer systems in the region (Podgorski et al., 2017). The main sources of aquifer recharge include rainfall and extensive irrigation rivers such as the Ravi River, the Jhelum River, the Sutlej River, the Chenab River and the Indus River in this area (Eqani et al., 2016; Podgorski et al., 2017). These homogenous, high transmissivity and unconfined aquifers are composed of sedimentary complex's and alluvial deposits, which mainly contained fine-average clay, sand and silt through varied extents of quartz, muscovite, biotite, chlorite and other minerals with an average thickness of 40 m (Mushtaq et al., 2018). The field sampling campaign was launched in November 2017, a total 146 groundwater samples in duplicates were randomly collected in Sindh ($n = 38$) and Punjab ($n = 108$) from the pre-existing boreholes (Fig. 1). The duplicate samples were filtered by using a 0.45 μm membrane (Whatman, USA) for quantification of major anions including SO_4^{2-} , PO_4^{3-} , NO_3^- , HCO_3^- , Cl^- , Br, SiO_2 and F⁻, while for measurement of cations such as Na⁺, K⁺, Mg^{2+} , Ca^{2+} , all samples were acidified with nitric acid (HNO_3^-). Then, the samples were stored in 50 mL propylene bottles tightly capped and stored at 4 °C by following the standard sampling protocols and methods defined by (APHA., 2005). The collected samples were transported to the "State Key Laboratory of Environmental Geochemistry, Chinese Academy of Sciences, Guiyang, China". To maintain and assure the quality and integrity of the samples, the critical quality control measures were taken during all the stages from samples' collection to analysis (APHA., 2005). Replicate samples were also collected to reduce cross-contamination during sampling, and all instruments were properly calibrated before analysis.

2.2. pH, EC, TDS, cations and anions analysis

pH and EC of the samples were measured on site by using pH/EC meter (HANNA instruments, Canada) and before sample analysis, the electrodes were properly calibrated. However, the TDS were measured indirectly by using EC values and conversion factor by using following equation (Moharir et al., 2002).

$$\text{Total dissolved solids (TDS mg/L)} = \text{Electric conductivity (EC } \mu\text{S/cm)} \times 0.64 \quad (1)$$

All the laboratory based chemical analysis was done at "State Key Laboratory of Environmental Geochemistry, Institute of Geochemistry of Chinese Academy of Sciences Guying, Guizhou Province, Republic of China". The analysis of major cations including Na⁺, K⁺, Mg^{2+} , and Ca^{2+} was performed by using Inductively Coupled Plasma Optical Emission Spectrometer (ICP-OES VISTA-MPX, Agilent, USA). The method was applied of metal flame photometer over specified ranges of wavelength. However, the major anions SO_4^{2-} , PO_4^{3-} , NO_3^- , HCO_3^- , Cl^- , Br, SiO_2 and F⁻ were

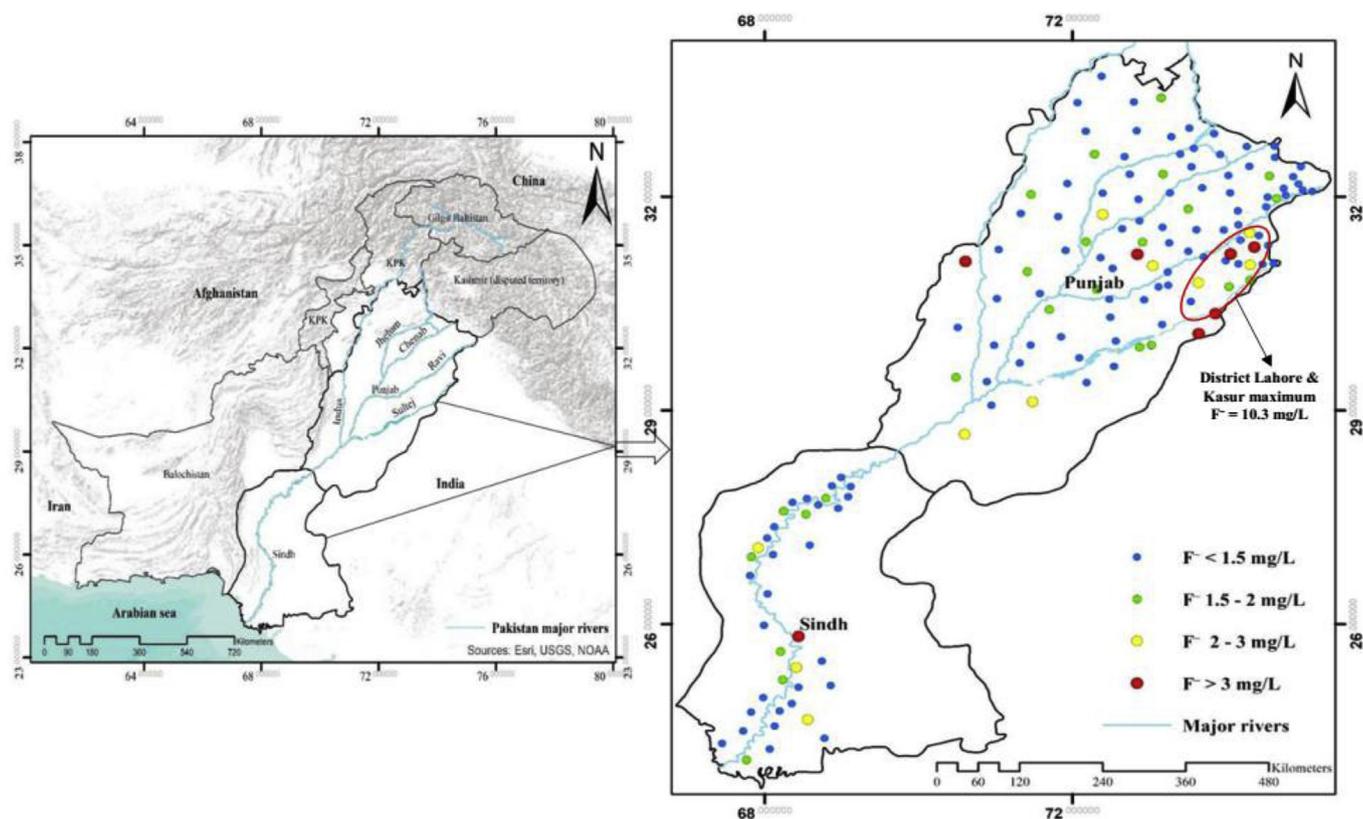


Fig. 1. Map of the study area showing the sampling points with $F^- < 1.5$ mg/L, $F^- 1.5\text{--}2$ mg/L, $F^- 2\text{--}3$ mg/L and $F^- > 3$ mg/L.

measured by Ion Chromatography System (ICS, DIONEX-90) ensuing USEPA method 300. Prior to chemical analysis, the instruments were properly calibrated with standards and method detection limits (MDL) were calculated as previously described (Kelly et al., 2005). The charge balance electro neutrality (EN %) of cations and anions in meq/L is certain to be within $\pm 5.0\%$.

2.3. Saturation indices

Saturation indices ($SI = \log [IAP/KT]$) were calculated for the current data to predict the mineralogy in the sampling area. Where, IAP = ion activity product (IAP) and KT = equilibrium constant of a precise mineral phases at room temperature. The SI values were measured by applying computer-based geochemical package PHREEQC (Interactive 2.11) and the WATEQF database.

2.4. Geological & statistical analysis

The study area maps were developed by using ArcGIS 10.3 (ESRI, USA). The principal component analysis (PCA) was performed for source distribution of physiochemical parameters. The PCA carried out through diagonalization matrix association; several problems that were arise from various numerical ranges of different variables in dataset are evaded and the variables were scaled mechanically on the variance and similarity basis (Jackson, 2005). Hydro-geochemical facies were determined through Chadha diagram (Chadha and Ray, 1999). All statistical analysis was performed by using XLSTAT (Addinsoft, USA) and SPSS 22 software (IBM, USA).

3. Results

3.1. Basic physico-chemical parameters, major ions

The results for basic physico-chemical parameters such as well depth pH, EC, TDS, F^- and major ions in groundwater samples from Sindh and Punjab are shown in (Table S1). The groundwater geochemistry of the present study area was also influenced by various well depth (m) and it was ranged from 27.4 to 61.0 m (mean = 34.8 m) in Sindh and 30.5–61.0 m (mean = 48.4 m) in Punjab (Fig. 2 a). The neutral to basic pH ranging from 7.3 to 8.7 and 7.1 to 9.0 were observed in samples from Sindh and Punjab, respectively with 34.2% and 28.4% of samples exhibited pH beyond WHO allowable range in groundwater (6.5–8.5) (Fig. 2 b). While, the EC varied from 656.7 to 3582.1 $\mu\text{S}/\text{cm}$ and 313.4 to 4925.4 $\mu\text{S}/\text{cm}$ (mean = 1491.8 and 1083.1 $\mu\text{S}/\text{cm}$) in Sindh and Punjab, respectively with 37.0% and 14.4% of samples had EC values beyond WHO standard value 1500 $\mu\text{S}/\text{cm}$. The TDS concentration ranged from 440.0 to 2400.0 (mean = 999.5 mg/L) and 210.0–3300.0 mg/L (mean = 725.6 mg/L) in groundwater samples of Sindh and Punjab, respectively (Fig. 2 c). Moreover, groundwater samples were observed mostly rich in Na^+ , Cl^- and poor in Ca^{2+} . The concentrations of Na^+ in groundwater samples from Sindh and Punjab, respectively ranged from 18.6 to 590.9 mg/L and 6.9–684.5 mg/L (mean = 185.2 and 145.7 mg/L), similarly for Cl^- , the concentrations were ranged 28.9–890.6 mg/L and 11.2–1057.6 mg/L (mean = 286.7 and 224.2 mg/L), while for Ca^{2+} , the concentrations ranged from 7.4 to 70.2 mg/L and 4.9–60 mg/L (mean = 31.3 & 29.1 mg/L) (Fig. 3 c, d & e). The other dominant anions were HCO_3^- and SO_4^{2-} (Fig. 3 a & b), whose concentrations ranged from 81.0 to 135.0 mg/L and 28.9–253.5 mg/L, (mean = 110.9 and 189.3 mg/L) and 18.4–435.4 mg/L and 2.9–304.6 mg/L with (mean = 138.0 and

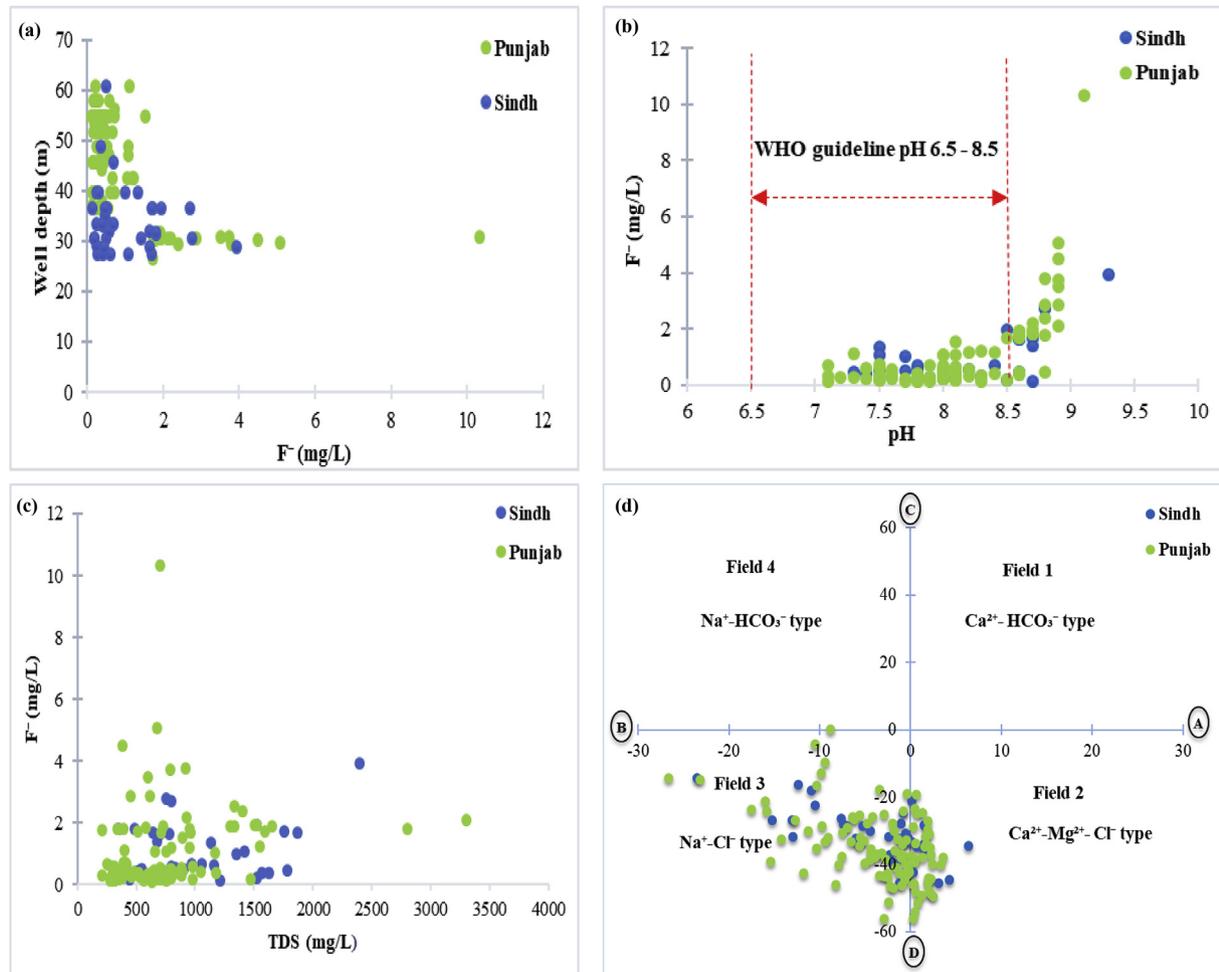


Fig. 2. Bivariate plots of F⁻ concentrations in groundwater with respect to well-depth (a) pH (b) TDS (c) and geo-chemical composition of groundwater of Sindh and Punjab (d).

82.4 mg/L) in groundwater of Sindh and Punjab, respectively. The Fig. 2 d highlighted the geochemistry of groundwater samples in term of Chadha plot that revealed Na⁺-Cl⁻ type and Ca²⁺-Mg²⁺-Cl⁻ water as pre-dominant types. The groundwater samples were observed highly sensitive towards the anthropogenic activities with highest NO₃⁻ concentration in Sindh ranged from 11.2 to 109.2 mg/L (mean = 48.5 mg/L) and in Punjab ranged from 7.5 to 92.7 mg/L (mean = 45.0 mg/L), Mg²⁺ ranged from 4.1 to 109.0 mg/L (mean = 35.9 mg/L) and 0.8–76.0 mg/L (mean = 20.6 mg/L), K⁺ ranged from 4.4 to 22.6 mg/L (mean = 9.6 mg/L) and 1.1–34.3 mg/L (mean = 7.1 mg/L) and low PO₄³⁻ concentration ranged from 0.01 to 0.02 mg/L (mean = 0.01 mg/L) and 0.01–0.4 mg/L (mean = 0.1 mg/L) respectively, (Fig. 3 g, i & j). However, the concentrations of Br and SiO₂ ranged from 0.01 to 1.7 mg/L (mean = 0.4 mg/L) and 14.7–35.3 mg/L (mean = 26.6 mg/L) in Sindh and 0.01–3.5 mg/L (mean = 0.3 mg/L) and 5.0–43.3 mg/L (mean = 24.8 mg/L) in Punjab, respectively.

3.2. Fluoride concentration variation in the study area

Overall F⁻ concentration in groundwater ranged from 0.1 to 10.3 mg/L (mean = 1.0 mg/L) and 27.4% samples revealed values exceeding the WHO permissible limit for F⁻ in groundwater 1.5 mg/L (Fig. 1). The F⁻ concentration in groundwater samples from Sindh and Punjab ranged from 0.1 to 3.9 mg/L (mean = 1.0 mg/L) and 0.1–10.3 mg/L (mean = 1.0 mg/L) with 28.9% and 26.6% samples

respectively, exceeding than WHO limit (Fig. 3 i & Table S1). The distinct pattern was observed in spatial distribution of F⁻ along the major rivers in Sindh and Punjab, as shown in Fig. 2a and b, c & d. Table S2 shows the Pearson's correlation coefficients between F⁻ concentration in groundwater with physico-chemical parameters, the Pearson's correlation coefficient values are also favoring the PCA (Table S3). Significant negative correlation was observed between F⁻ and well-depth ($r = -0.2$), and positive with pH ($r = 0.8$), TDS and EC ($r = 0.2$). The pattern of F⁻ distribution in study area was clustered as follows: 1) the shallow depth, brackish Na⁺-Cl⁻ type of water, alkaline pH > 8.5 with high F⁻ content in groundwater in Sindh area in which the F⁻ level is normally above than 3 mg/L and Punjab (Lahore and Kasur zone) exceeding than 4 mg/L, 2) the shallow medium, at pH ranged 7.5 to 8.5 the F⁻ concentration in Sindh and Punjab higher than 1.5 mg/L and less than 2.5 mg/L and higher than 2 and less than 4 mg/L respectively, 3) deep groundwater pH < 7.5 the F⁻ concentration less than 1.5 mg/L in Sindh and Punjab respectively. Likewise, the Pearson's correlation coefficients of F⁻ concentration in groundwater with major ions observed as, F⁻ and Na⁺ ($r = 0.2$), F⁻ and K⁺ ($r = 0.2$), F⁻ and Ca²⁺ ($r = -0.2$), F⁻ and Cl⁻ ($r = 0.2$) and F⁻ and NO₃⁻ ($r = -0.2$) (Table S2).

3.3. Saturation indices of the study area

The mineral index, gypsum, calcite, dolomite and fluorite in groundwater samples present are plotted (Fig. 9). The SI = >

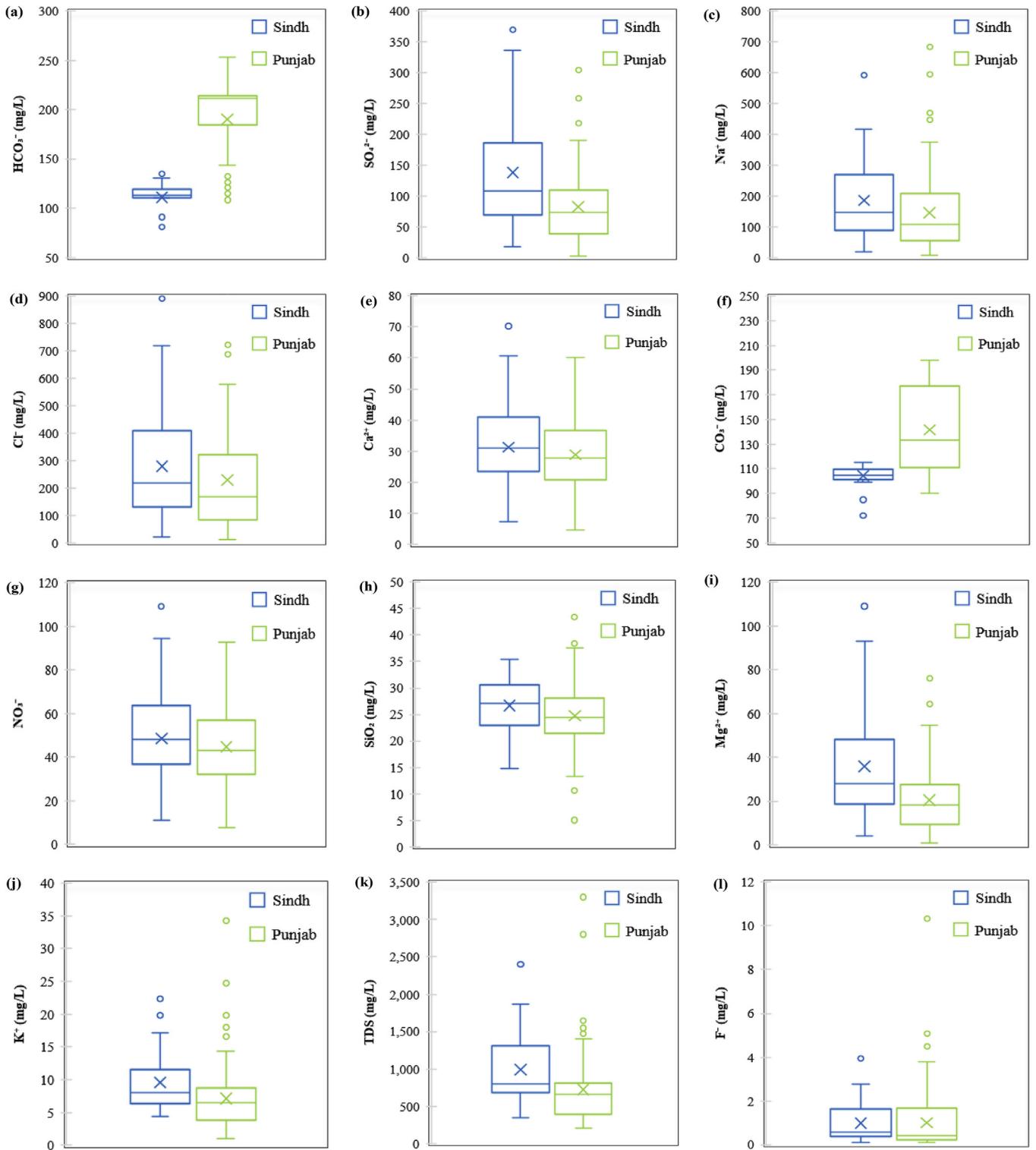


Fig. 3. Box plots showing the summary of investigated parameters HCO_3^- (a), SO_4^{2-} (b), Na^+ (c), Cl^- (d), Ca^{2+} (e), CO_3^{2-} (f), NO_3^- (g), SiO_2 (h), Mg^{2+} (i), K^+ (j), TDS (k) and F^- (l) groundwater samples collected from Sindh and Punjab study.

0 indicates the precipitation is needed as to achieve equilibrium and $\text{SI} < 0$ suggests that groundwater is under saturated state and dissolution is required as to reach equilibrium state. The results for variation of minerals distribution in the study area are summarized in (Table S1).

4. Discussion

4.1. Groundwater quality & major hydrogeochemical process

The EC is a well-known indicator of salt content in groundwater (Noli and Tsamos, 2016). The EC of groundwater depends on aquifer

recharge sources such as recharge from freshwater resources including rivers, rainfall or irrigation water returns (Argamasilla et al., 2017). The direct disposal of industrial, agricultural and household wastes into riverine system of Pakistan may be the major cause of high EC and TDS in groundwater from Sindh and Punjab. Pervious literature also reported the same sources of elevated EC in groundwater samples from Sindh and Punjab (Brahman et al., 2013; Farooqi et al., 2007; Mushtaq et al., 2018; Podgorski et al., 2017; Rasool et al., 2015; Shahid et al., 2018). The elevated concentration of EC reported associate to the higher concentration of TDS in groundwater in the presences of cations and anions, as previously described (Ali et al., 2018b; Farooqi et al., 2007; Tabassum et al., 2018). Whereas (Tirkey et al., 2017), suggested that the presence of higher TDS content in groundwater is also due to the inorganic and organic dissolution of minerals in aquifer system. However, the various suite of main geochemical processes might be occurring in the current study area as highlighted in our results by the variation in spatial distribution of F⁻ and major ions. The Gibb's plots (Gibbs, 1970) were used to categorize the sources of possible geochemical reactions in groundwater of Sindh and Punjab (Fig. 4 a & b). The 90.0% samples from the study area fall in rock-water dominance zone, suggesting mineral weathering as the significant mechanism that controlled groundwater chemistry. Whereas, remaining 10.0% samples fall in evaporation-crystallization zone that might be attributed to the evaporation/dissolution effects or both involved in the formation saline groundwater in the study area. While the samples fall in rock-water dominant zone indicated weathering and dissolution of minerals as main sources of chemical interactions in deep groundwater aquifer (Ali et al., 2018a; Farooqi et al., 2007; Rafique et al., 2015). The groundwater receives ions during the dissolution of minerals from sediments or soil through rock-water interaction. The bivariate plots were used to assess specific view of mineral weathering in groundwater system (Fig. 5). To assess the main controlling lithology in the present study, Na⁺ standardized ratios (Ca²⁺/Na⁺, HCO₃⁻/Na⁺ & Mg²⁺/Na⁺) were calculated by following method previously described by (Li et al., 2018). The Fig. 5 a & b shows, the samples fall near the carbonate-silicate weathering line and silicate dominant area, suggesting the silicate dissolution also played significant role in groundwater geochemistry in the present study area. For understanding the contribution of carbonate weathering in groundwater geochemistry, the graph between Ca²⁺ + Mg²⁺ against HCO₃⁻ + SO₄²⁻ was plotted. Whereas, Fig. 5 c suggest the groundwater, samples fall below 1:1 line, indicating the carbonate and gypsum mineral dissolution was occurred in the groundwater. While the samples away from the line suggesting prevalence of (HCO₃⁻ + SO₄²⁻) against (Ca²⁺ + Mg²⁺). However, these results highlighted gypsum and carbonate not the main sources of geochemical processes in the present sampling locations, the points away from the line, may be attributed to the presence of Ca²⁺ and Mg²⁺ in groundwater primarily originated from cation exchange or SiO₂ dissolution (Brahman et al., 2013; Farooqi et al., 2007; Kumar et al., 2006; Li et al., 2018). The Fig. 5 d shows gypsum dissolution in aquifer through binary plotting of Ca²⁺ + Mg²⁺ - 0.5 HCO₃⁻ versus SO₄²⁻ as showed in previous studies (Li et al., 2018). Almost all data points fall above zero line provided the strong evidence that the gypsum mineral dissolution is the key source of geochemical interactions in groundwater of the current study area (Fig. 5 d). However, significant evaporative effects were also prevalent in the study area, the contribution of halite dissolution is assessed through plot between Na⁺ and Cl⁻ (Tabheri et al., 2017). The Fig. 5 e shows the strong positive correlation between Na⁺ and Cl⁻ further suggesting the natural dissolution of evaporative minerals (Halite) in these arid and semi-arid regions, as reported in previous study (Mushtaq et al., 2018).

4.2. Sodium percentage and absorption ratio-based water classification

The sodium percentage (Na⁺%) is an important parameter in all type of natural water, and it is used to measure the suitability of water for agricultural purpose (Nakhaei et al., 2016; Wilcox, 1958). The elevated Na⁺ % may causes de-flocculation and damage soil tilth and permeability (Nakhaei et al., 2016). The Na% in groundwater area calculated through the following equation:

$$\text{Na}\% = \text{Na}^+ + \text{K}^+ / (\text{Ca}^{2+} + \text{Mg}^{2+} + \text{Na}^+ + \text{K}^+) \times 100 \quad (2)$$

whereas Na⁺, K⁺, Ca²⁺ and Mg²⁺ concentrations in groundwater are expressed in meq/L. The Wilcox diagram Fig. 6 a showed the 2.7%, 21.0% and 25.0% samples fall in unsuitable, doubtful and permissible to doubtful fields, respectively. While, the rest of samples fall in good to permissible and very good to good fields. For irrigation purpose, the Na⁺ or alkali level in groundwater is measured through the total and comparative concentration of major cations and expressed as sodium absorption ratio (SAR) (Nakhaei et al., 2016). The SAR is also used to assess the suitability of groundwater agricultural irrigation, because excess concentration of Na⁺ in groundwater causes to reduce the soil permeability as well as soil structure (Brahman et al., 2013). The sodium hazard measured through SAR by following equation (Islam et al., 2017).

$$\text{SAR} = \text{Na}^+ / \text{Ca}^{2+} + \text{Mg}^{2+} / 2 \quad (3)$$

The SAR values in the present study areas Sindh and Punjab ranged from 0.2 to 5.6 (mean = 1.2) and 0.1 to 5.3 (mean = 1.1) with elevated Na⁺ and low Ca²⁺ concentrations respectively, (Table S1). The elevated Na⁺ concentration in groundwater could reflect the dissolution of the lithogenic Na⁺ and to exchange its ions for dissolved Ca²⁺ through clay minerals in aquifer system (Rafique et al., 2015). On the basis of United States (US) salinity hazard diagram the graph was plotted between SAR and EC as reported in previous study (Fig. 6 b) (Nakhaei et al., 2016). The plot illustrated that the groundwater samples from the present study area fall in C1–S1, C2–S1 and C3–S1 zones suggesting low, medium and high salinity, while C4–S1 indicating very high salinity with low Na⁺ type, which confirmed the halite dissolution as significant source of salinity in these samples. For further classification, Van Wirdurm's plot was drawn between the ionic ratios (IR) of Ca²⁺ and Cl⁻ (meq/L) against EC (Van Wirdurm, 1980). The ionic ratio (IR) values calculated by following equation:

$$\text{IR} = [\text{Ca}^{2+}] / ([\text{Ca}^{2+}] + [\text{Cl}^-]) \quad (4)$$

The IR values measured as the occurrence of Ca²⁺ and Cl⁻ between major cations and anions. The EC measured as an indicator of salinity. The Van Wirdurm's plot Fig. 6 c showed about 42% groundwater samples fall in atmospheric (At) zone and the rest of samples fall in lithotrophic (Li) zone with high salinity. The plot suggested high salinity in these samples that could be attributed to the halite dissolution of saline sediments.

4.3. Mechanism and sources of F⁻ in groundwater

4.3.1. Alkaline conditions, adsorption and anthropogenic activities

The relationship between F⁻ major ions as well as physico-chemical parameters (pH, EC, TDS & well depth) also revealed various geochemical process that control F⁻ concentration in groundwater. Whereas, the Fig. 2 b, Table S2 expressed a strong correlation between F⁻ and pH, and alkaline environmental conditions that promoted F⁻ leaching through desorption or by ion

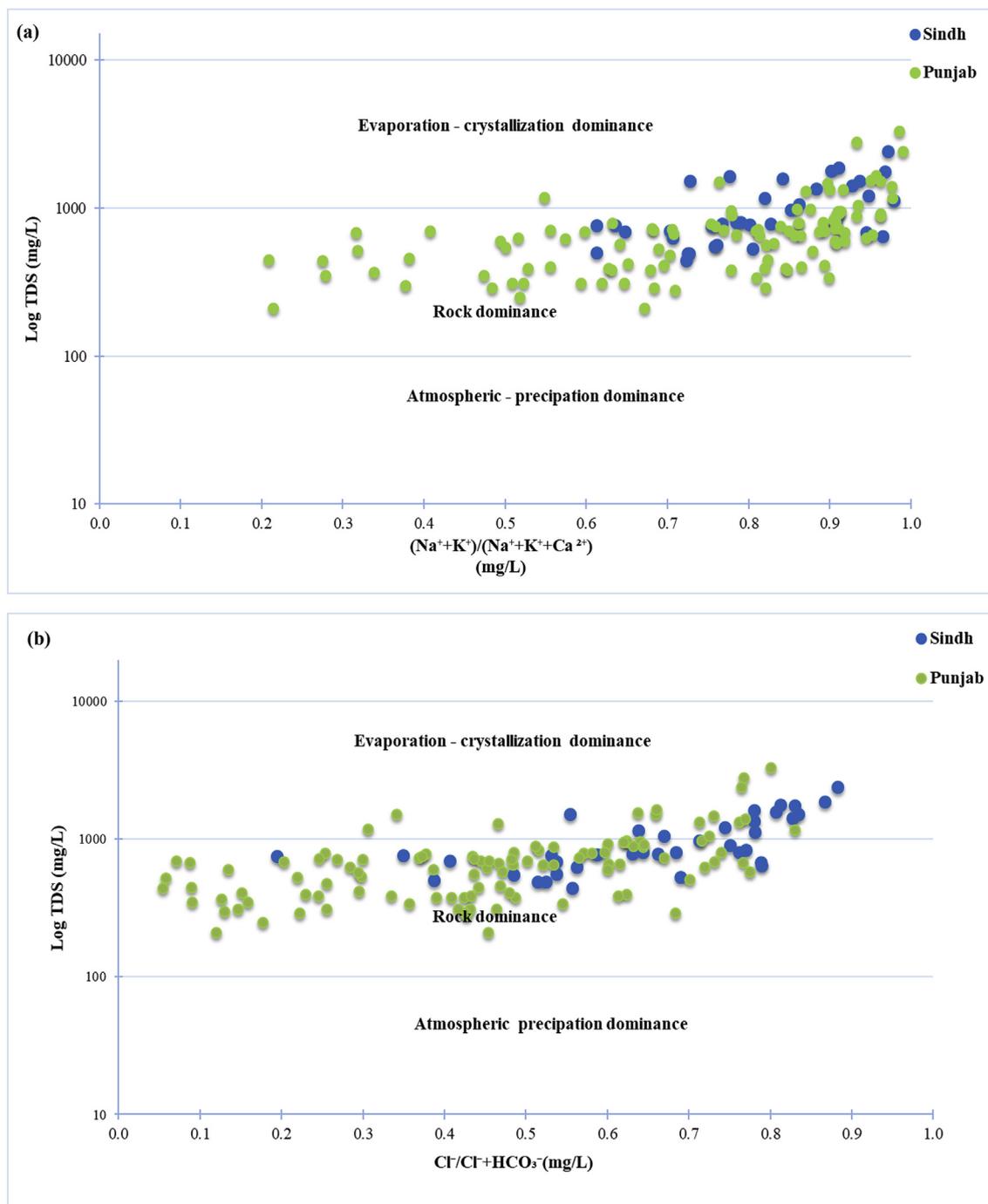


Fig. 4. Gibb's plots showing the geochemical mechanisms of groundwater chemistry: log TDS versus $Na^+ + K^+ / Na^+ + K^+ + Ca^{2+}$ (a) and log TDS vs $Cl^- / Cl^- + HCO_3^-$ (b).

exchange process (Luo et al., 2018; Magesh et al., 2016). The pH increased from the zero-point charges of the sorbents in aquifer sediments, resulting in desorption of F^- in groundwater. The basic pH conditions in aquifer system promoted solids with negatively or neutrally charged surface that caused the desorption of F^- to $F-OH$ ion exchange (Li et al., 2018). The F^- ion exchange ($F-OH$) and F^- release in groundwater took place under basic conditions (Vithanage et al., 2014). The alkaline environmental conditions in the present study area indicated the abundance of (OH^-) minerals (Nouri et al., 2006), known as apatite muscovite, amphiboles and biotite, which could be major possible source of elevated F^- in groundwater. The previous studies revealed that these minerals

comprised a significant amount of exchangeable F^- (Jacks et al., 2005; Li et al., 2018). However, in most groundwater samples, the positive relation was also observed between F^- and HCO_3^- which suggested the competitive absorption and weathering as contributing factors in F^- desorption in groundwater (Fig. 6 a, Table S2) (Rafique et al., 2015; Vázquez-Guerrero et al., 2016). The presence of HCO_3^- ions in groundwater decrease the number of available adsorbents sites that can lead to release F^- from deposits or weathering of silicate and carbonate minerals such as calcite or dolomite produce bulk of F^- and HCO_3^- and consequently enhance F^- concentration in groundwater. While, higher level of HCO_3^- in groundwater has minute effect on F^- concentration but the positive

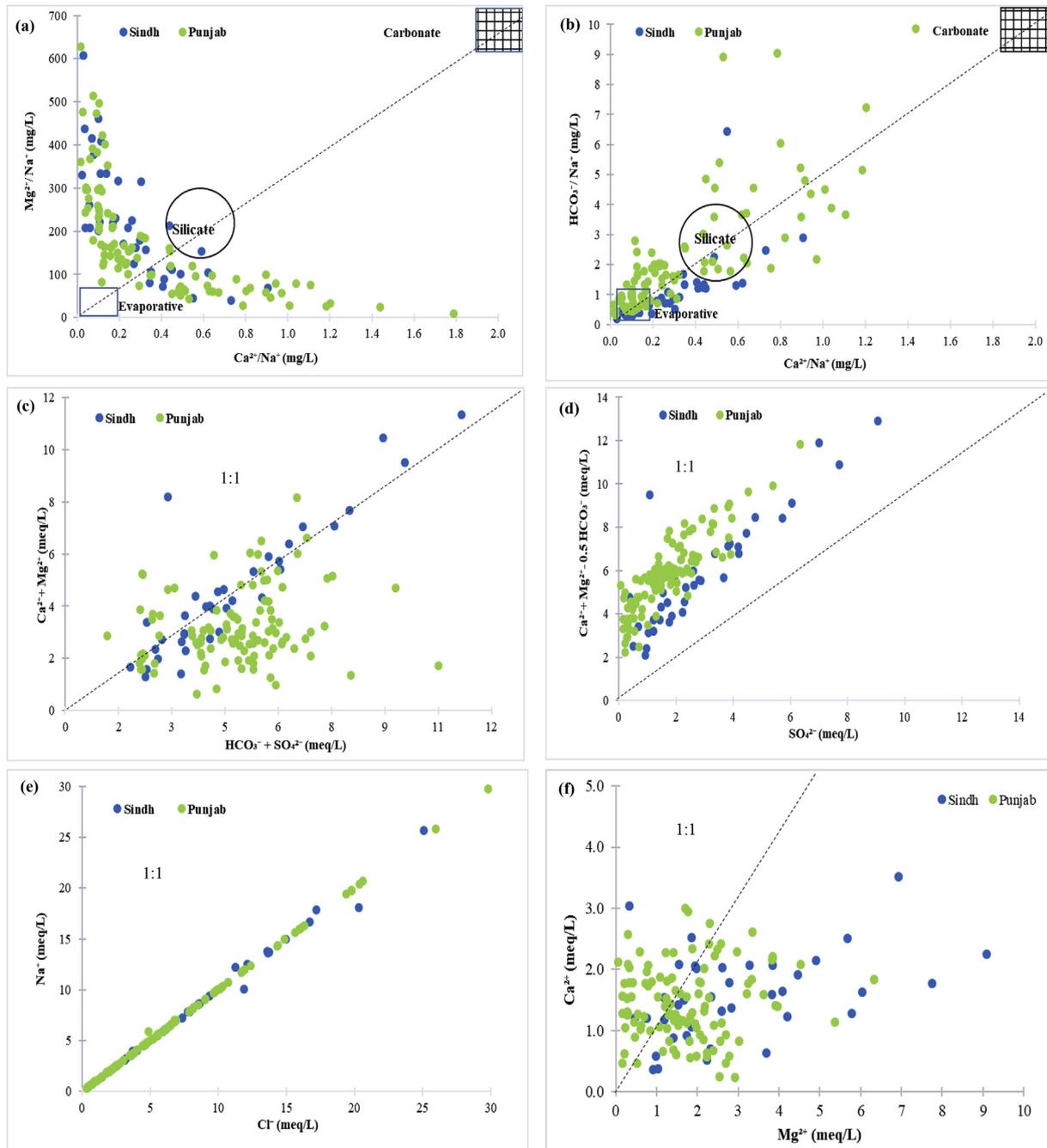


Fig. 5. Scattered plots of major ions showing the main sources of chemical in the study area Sindh and Punjab. Plots showing the mineral weathering; Mg^{2+}/Na^+ vs Ca^{2+}/Na^+ (a), HCO_3^-/Na^+ versus Ca^{2+}/Na^+ (b), plots showing the extend carbonate and dolomite minerals dissolution; $Ca^{2+} + Mg^{2+}$ versus $HCO_3^- + SO_4^{2-}$ (c), plot suggesting gypsum mineral dissolution; $Ca^{2+} + Mg^{2+} - 0.5 HCO_3^-$ versus SO_4^{2-} (d), graph shows the halite dissolution; Na^+ versus Cl^- (e) and Ca^{2+} versus Mg^{2+} .

correlation between F^- and HCO_3^- suggests the $F^- - HCO_3^-$ mechanism is also prevailing in the current study area. The weak positive relation between F^- versus NO_3^- (Fig. 6 e, Table S2). The elevated concentration of NO_3^- higher than 5 mg/L in natural water indicated the influence of anthropogenic activities such as fertilizers and wastes from agricultural, domestic and industrial sources (Li et al., 2018). The infiltration of fertilizers from soil to aquifer system facilitated enrichment of F^- in natural water through leaching/direct input of F^- (Sharma and Subramanian, 2008). The weak correlation between F^- and NO_3^- in the present study also suggested relatively mild impact of anthropogenic activities on F^- concentration in groundwater.

4.3.2. Evaporation, evaporative dissolution and salt effects on fluoride

Evaporation is also considered as a main mechanism for precipitated elimination of Ca^{2+} from the groundwater and caused F^- enrichment (Alarcón-Herrera et al., 2013; Li et al., 2018). Through evaporation process the water change to vapor that may lean towards increased level of F^- as well as other chemical species in groundwater. Though, the significant increase in Ca^{2+} level caused through evaporation process that lead towards extensive precipitation of calcite, hence promoting F^- enrichment in natural groundwater (Li et al., 2015; Li et al., 2018). For further understanding of the evaporation effect on F^- enrichment, a plot was

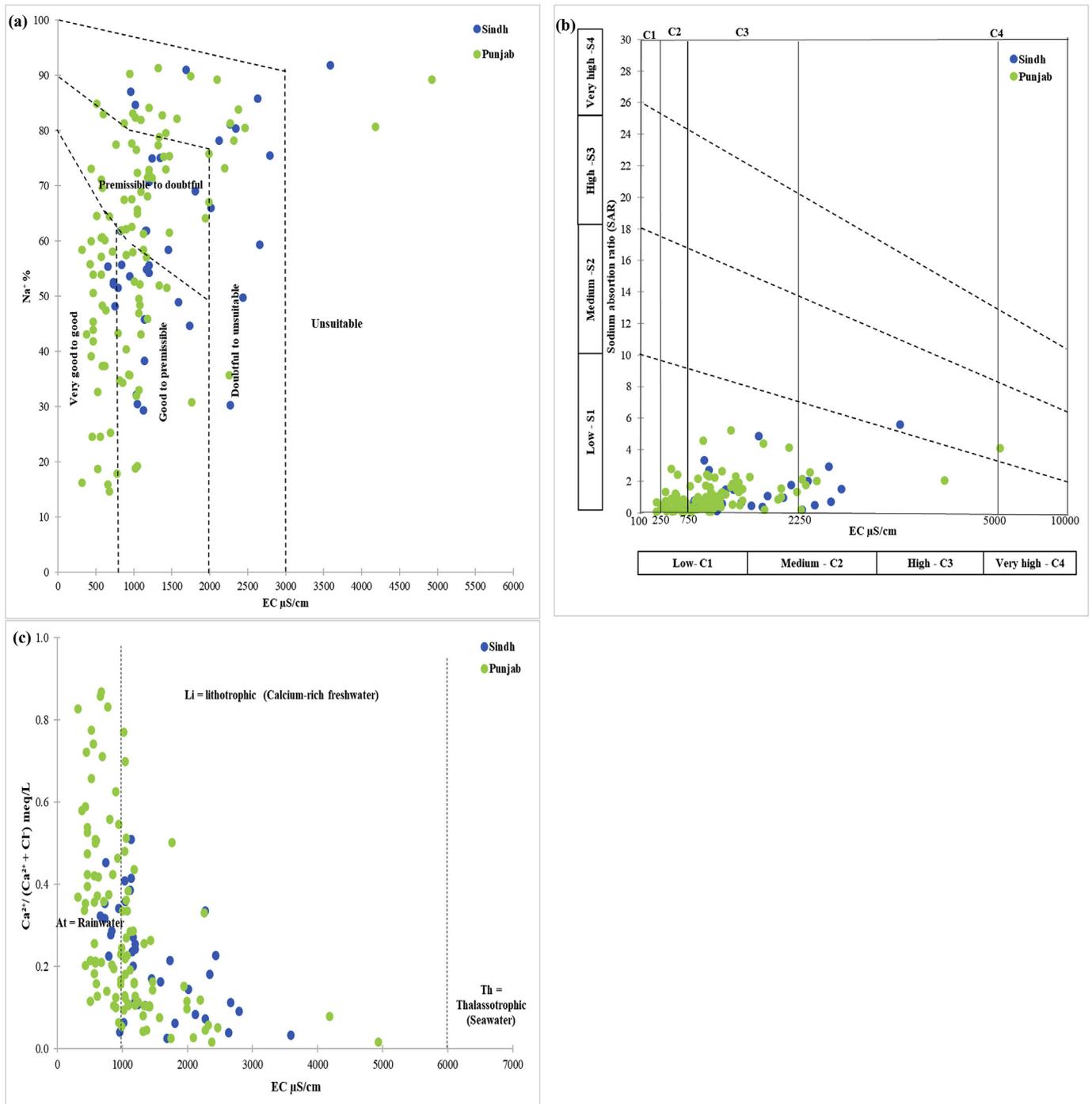


Fig. 6. Groundwater quality classification with respect to Na% vs EC ($\mu\text{S}/\text{cm}$) (a), salinity hazard graph between sodium absorption ratio (SAR) versus EC ($\mu\text{S}/\text{cm}$) (b) and Van Wirdurm's graph to classify groundwater with respect to rainwater (At), lithotrophic (Li) and thalassotrophic or seawater interference $\text{Ca}^{2+}/\text{Ca}^{2+} + \text{Cl}^{-}$ versus EC ($\mu\text{S}/\text{cm}$) (d).

developed between $\text{F}^{-}/\text{Cl}^{-}$ ratios in meq/L versus F^{-} mg/L (Fig. 7 a). The evaporation enriched F^{-} and $\text{F}^{-}/\text{Cl}^{-}$ ratios in meq/L likely remained stable (Olaka et al., 2016). The dissolution of F^{-} bearing minerals also contributed in F^{-} enrichment of groundwater. The Chadha's plot showed almost 72.6% sample dominated by $\text{Na}^{+}-\text{Cl}^{-}$ type of water and confirmed that the halite dissolution process was a major contributor for F^{-} enrichment in groundwater (Fig. 8 a & b). Further investigation highlighted the dissolution of evaporative minerals could be another source of F^{-} in groundwater. During the evaporation process, F^{-} can be precipitated with various salts in the

form of crystalline solids throughout evaporation or decrease in water table (Li et al., 2018). As shown in Fig. 5 a to e, the evaporative dissolution occurred in the present study area, mainly in shallow groundwater, F^{-} comparatively originated from leaching evaporites through precipitation, irrigation returns water or surface water. The previous studies also reported the effects of salts on F^{-} concentration in groundwater from the present study area (Brahman et al., 2013; Farooqi et al., 2007; Rafique et al., 2015; Rasool et al., 2017; Rasool et al., 2015). In alluvial aquifer system, the higher ionic strength could raise the solubility of F^{-} - bearing mineral deposits. In

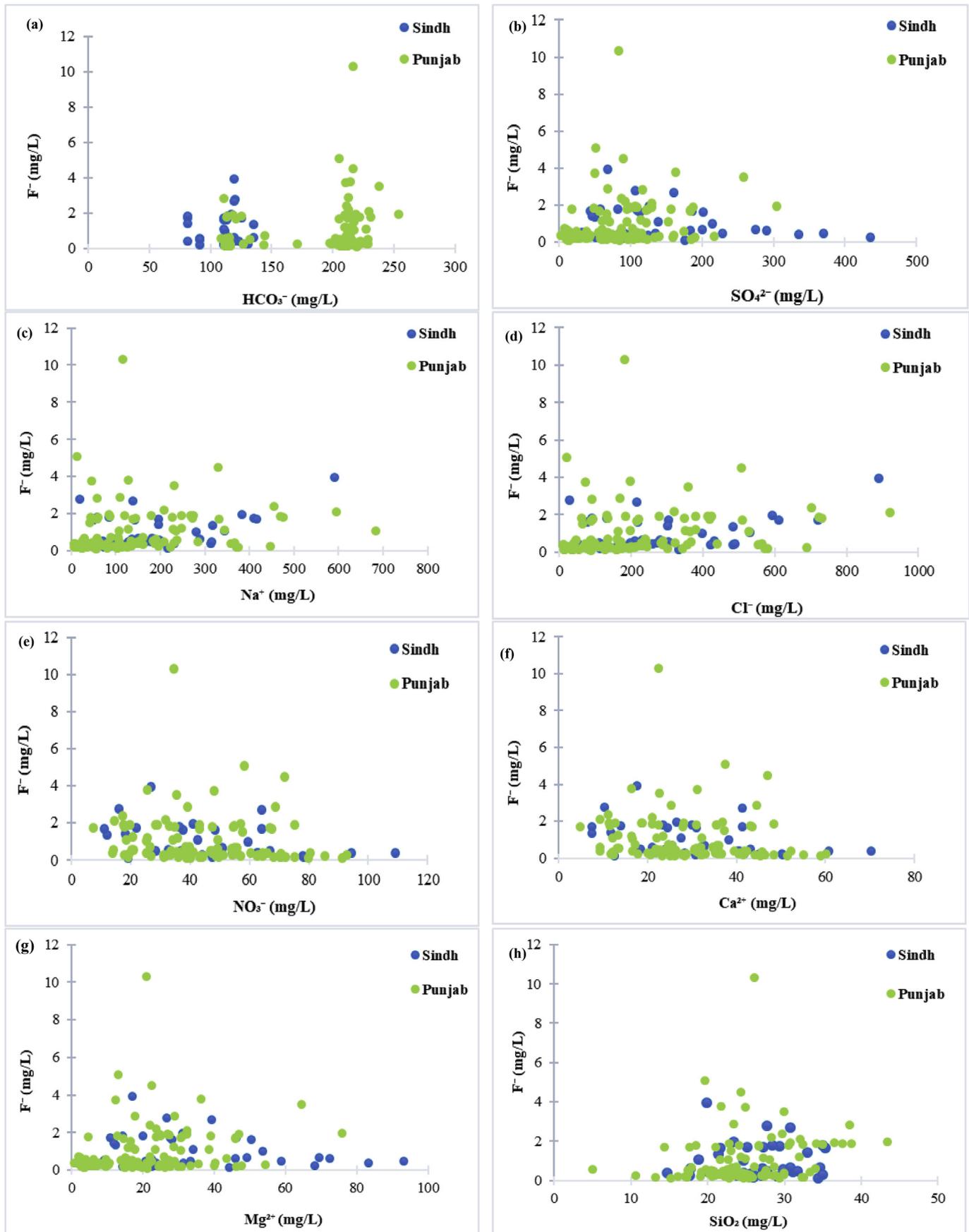


Fig. 7. The bivariate plots showing F^- variation with respect to geochemical parameters F^- versus HCO_3^- (a), F^- versus SO_4^{2-} (b), F^- versus Na^+ (c), F^- versus Cl^- (d), F^- versus NO_3^- (e), F^- versus Ca^{2+} (f), F^- versus Mg^{2+} and F^- versus SiO_2 in groundwater samples of Sindh and Punjab.

the present study area, Na^+ , Cl^- and SO_4^{2-} concentration revealed positive correlations with F^- , which suggested the significant effect of salinity on F^- levels in groundwater (Fig. 6 b to, Table S2). The elevated salt content (Na^+Cl^- and $\text{Na}^+\text{SO}_4^{2-}$) in groundwater may cause substantial decrease in saturation indices (SI) of fluorite level in groundwater (Gao et al., 2007; Li et al., 2018). However, high salinity level decreases the SI content of fluorite and boost up dissolution process of F^- - bearing mineral deposits that ultimately increases F^- level in groundwater. The negative correlation between Ca^{2+} , Mg^{2+} and F^- indicated fluorite controlling factor (CaF_2) associated dissolution of the F^- and elimination of Ca^{2+} from groundwater (Fig. 7 f & g, Table S2). The other mechanisms such as the dolomite/gypsum dissolution or cation exchange could cause the removal of Ca^{2+} from groundwater (Barzegar et al., 2017).

4.4. Saturation indices

The saturation indices (SI) of all groundwater samples from the present study area are given in Fig. 9. The SI of calcite, fluorite, dolomite and gypsum provided detailed understanding and mechanisms of fluorite dissolution that commonly enhanced through precipitation of calcite (Brahman et al., 2013). The Fig. 9 a highlighted the simultaneous increase of SI calcite and SI dolomite form negative to positive zone suggesting the dissolution of calcite and dolomite and these minerals possibly precipitated in the groundwater, both in Sindh and Punjab. However, the inactive kinetics of dolomite reported to be insufficient for the magnesium carbonate to precipitate (Bozdağ, 2016; Li et al., 2018). The $\text{Ca}^{2+}/\text{Mg}^{2+}$ ratios have been used to assess an index to the dissolution of dolomite and calcite minerals in aquifer (Fig. 5 e) (Li et al., 2018). The $\text{Ca}^{2+}/\text{Mg}^{2+}$ ratio >1 suggested the calcite dissolution dominance and ratio <1 indicated the dissolution of dolomite minerals prominence in groundwater (Sheikhy Narany et al., 2014). As shown in Fig. 5 e, the 70% samples from present study fall below 1:1 line, suggesting the dolomite minerals dissolution was dominant. While the rest of samples fall above 1:1 line that indicated the calcite mineral dissolution was also prevailing in the study area. The 84.2% samples from Sindh Province fall below line that confirmed the dolomite dissolution as main process to control groundwater chemistry in Sindh, compared to those of Punjab. In a nutshell the dolomite dissolution increased Ca^{2+} and Mg^{2+} concentration in groundwater. Therefore, initiated the precipitative elimination of Ca^{2+} as calcite. However, Mg^{2+} continually dissolved in groundwater. Based on $\text{Ca}^{2+}/\text{Mg}^{2+}$ ratio, the dolomite minerals dissolution influenced on groundwater chemistry. Compare with Punjab, the groundwater samples from Sindh gained more chemicals from dolomite minerals dissolution than other mechanisms. The precipitative Ca^{2+} removal carried out through gypsum dissolution (Li et al., 2018) and generated an extra Ca^{2+} that caused gypsum dissolution (Rezaei et al., 2017). As shown in Fig. 9 c & e, the SI of calcite versus Ca^{2+} and SI dolomite against Mg^{2+} , most of the samples fall above line suggesting that the samples are saturated with calcite and dolomite dissolution could increase Ca^{2+} and Mg^{2+} concentration in groundwater. While, the SI of gypsum versus SO_4^{2-} represented the undersaturated samples. The SI calcite versus the SI gypsum and the SI dolomite lead to the simultaneous gypsum dissolution and calcite precipitation in groundwater from both Sindh and Punjab (Fig. 9 b & d). A plot between the SI calcite against the SI fluorite the Fig. 9 g showed the relationship between fluorite and calcite in aquifer system, as previously described (Farooqi et al., 2007). While, the 80.3% samples from both Sindh and Punjab revealed negative values for the SI fluorite and positive value for the SI calcite suggested the groundwater samples undersaturated with fluorite, while saturated with calcite. Therefore, limited influence of calcite mineral dissolution/precipitation observed on F^-

concentration in groundwater samples from the present study area. Hence, F^- concentration in groundwater depends on interaction, rate and frequency of F^- - bearing minerals. The present status of fluorite dissolution (other than SI) were sensitive with respect to Ca^{2+} level in groundwater. In groundwater, calcite played a significant role to control Ca^{2+} level (Fig. 9 c), dissolution of F^- -bearing minerals and F^- concentration (Brahman et al., 2013; Farooqi et al., 2007; Li et al., 2018; Singaraja et al., 2014). The graph between the SI of fluorite versus F^- (mg/L) provided another angle to understand association between fluorite and F^- in groundwater system (Fig. 9 h) (Brahman et al., 2013). The positive correlation observed between elevated F^- samples with fluorite in both Sindh and Punjab, which implied that the fluorite dissolution may also play significant role for leaching of F^- in groundwater from sediments.

4.5. Principle component analysis

The principal component analysis (PCA) is a best statistical recognition method that describes variance of large data set of variables to small set of independent variables on base of inter-correlation (Dupas et al., 2015). The five-principle components (PC-1, PC-2, PC-3, PC-4 & PC-5) were analyzed from present dataset showed 74.23% of the total variance on the resulted data obtained after analysis of groundwater samples taken from both Sindh and Punjab (Table S3). The positive score of loading principle components suggesting groundwater samples are influenced by the significantly loaded water variables. Whereas, the negative loading score shows the groundwater quality is unfaceted by those variables. The PC-1 explained 29.8% variance of total dataset of the groundwater parameters including major ions Na^+ , K^+ , Mg^{2+} , Cl^- , SO_4^{2-} , Br and F^- and physico-chemical parameters well depth, pH, EC and TDS. Except well depth, the physico-chemical parameters almost behaved equally as important as major cations, anions and F^- concentration in groundwater. The PC-1 suggesting the ionic composition of groundwater controlling by weathering, minerals dissolutions and ion exchange process. Overall both natural and human related sources play important role in groundwater pollution. The Na^+ , K^+ , Mg^{2+} , Br and Cl^- and were originated from the natural sources such as weathering of granitic rocks, ion exchange process and dissolution of plagioclase, albite, dolomite and muscovite, fluorite and halite dissolution process drive F^- enrichment in groundwater (Kaown et al., 2009; Li et al., 2015; Soltermann et al., 2016). Whereas, Cl^- and SO_4^{2-} contamination in groundwater also cause from the anthropogenic activities i.e., agricultural activities, industrial effluent, atmospheric deposition and soil sources (Rashid et al., 2019). Moreover, the physico-chemical parameters pH, EC and TDS pollution sources also attribute towards the alteration of sulfide bearing minerals as well as anthropogenic activities (Rashid et al., 2019). The PC-2 explained 16.2% of variance between Ca^{2+} and NO_3^- and concentrations in groundwater, possible sources the dissolution of calcite minerals and NO_3^- comes from agricultural activities such as widely use urea and animal manure for purpose to increase soil fertility (Farooqi et al., 2007; Rashid et al., 2018). The PC-3 explained 12.1% of variance with strong positive loading with HCO_3^- , CO_3^{2-} , Ca^{2+} and with well depth. Natural sources dissolution calcium carbonate (CaCO_3) concentration increase with well-depth contributes towards Ca^{2+} and HCO_3^- the contamination (Rashid et al., 2019) in aquifer system of the present study area. The PC-4 and PC-5 explained 9.2% and 7.1% variance with significant correlation coefficient value SiO_2 , PO_4^{3-} and pH respectively. The PO_4^{3-} and SiO_2 pollution in groundwater natural sources included silicate weathering, dissolution of phosphate rocks and sulfide ores (Rashid et al., 2018; Srinivasamoorthy et al., 2008). From the above observation one can clearly understand the sample distribution and their

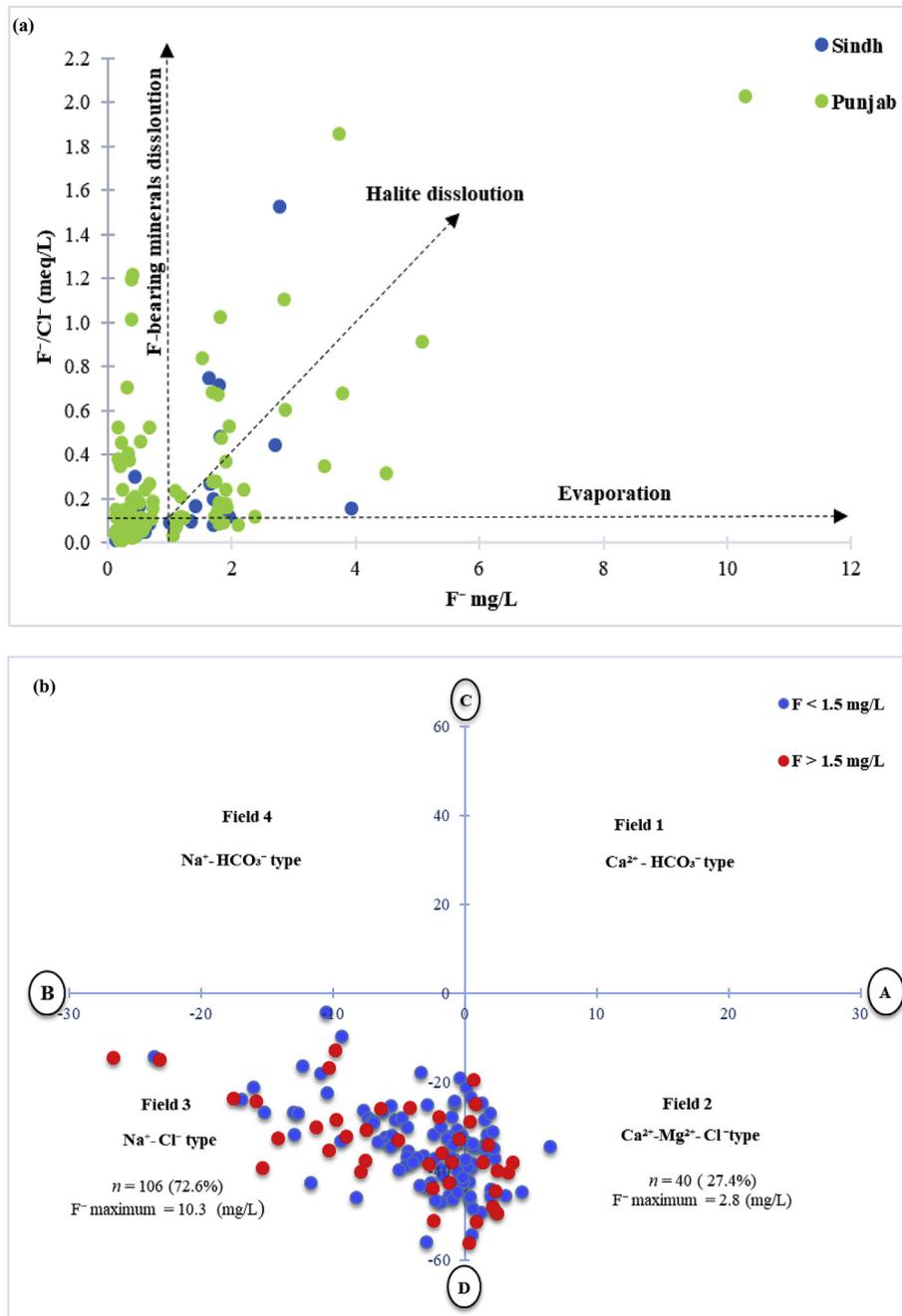


Fig. 8. Plot between F^-/Cl^- versus F^- concentration in groundwater shows the different evaporation effects (a) and Chad's plot showing over all groundwater chemistry with respect to F^- in groundwater samples in the study area (b).

characteristics. Importantly, PC-1 was more enriched and had strong positive correlation with pH, EC, TDS, Na^+ , K^+ , Mg^{2+} , Cl^- , SO_4^{2-} , Br and F^- . The positive correlation between EC and TDS is a well-known indicator for the presences of elevated ions such as Na^+ , K^+ , Mg^{2+} , Cl^- and Br that reported to be mainly responsible for soluble salts in groundwater (Chanpiwat et al., 2011). The presences of soluble salts and alkaline environment promoted the halite dissolution and other minerals weathering process that ultimately caused F^- enrichment in groundwater of the present study area.

5. Conclusion

The present study highlighted F^- contamination in groundwater

prevailing with different pattern in unconfined aquifer system along the major rivers of Sindh and Punjab, Pakistan. A total of 28.9% and 26.6% groundwater sample respectively in Sindh and Punjab exhibited F^- concentration beyond its WHO limit (1.5 mg/L). Importantly, several geochemical processes were identified that were possibly involved in F^- enrichment of unconfined aquifers such as minerals weathering, alkaline environmental, dolomite dissolution, arid climatic conditions and fluorite dissolution. While, 72.6% sample from each Sindh and Punjab dominated with $Na^+ - Cl^-$ type of water, confirmed that the halite dissolution process as the major contributor for F^- enrichment in groundwater of the present study area. In a nutshell, the alkaline conditions, evaporation effect or dissolution of the evaporative, F-bearing minerals dissolution,

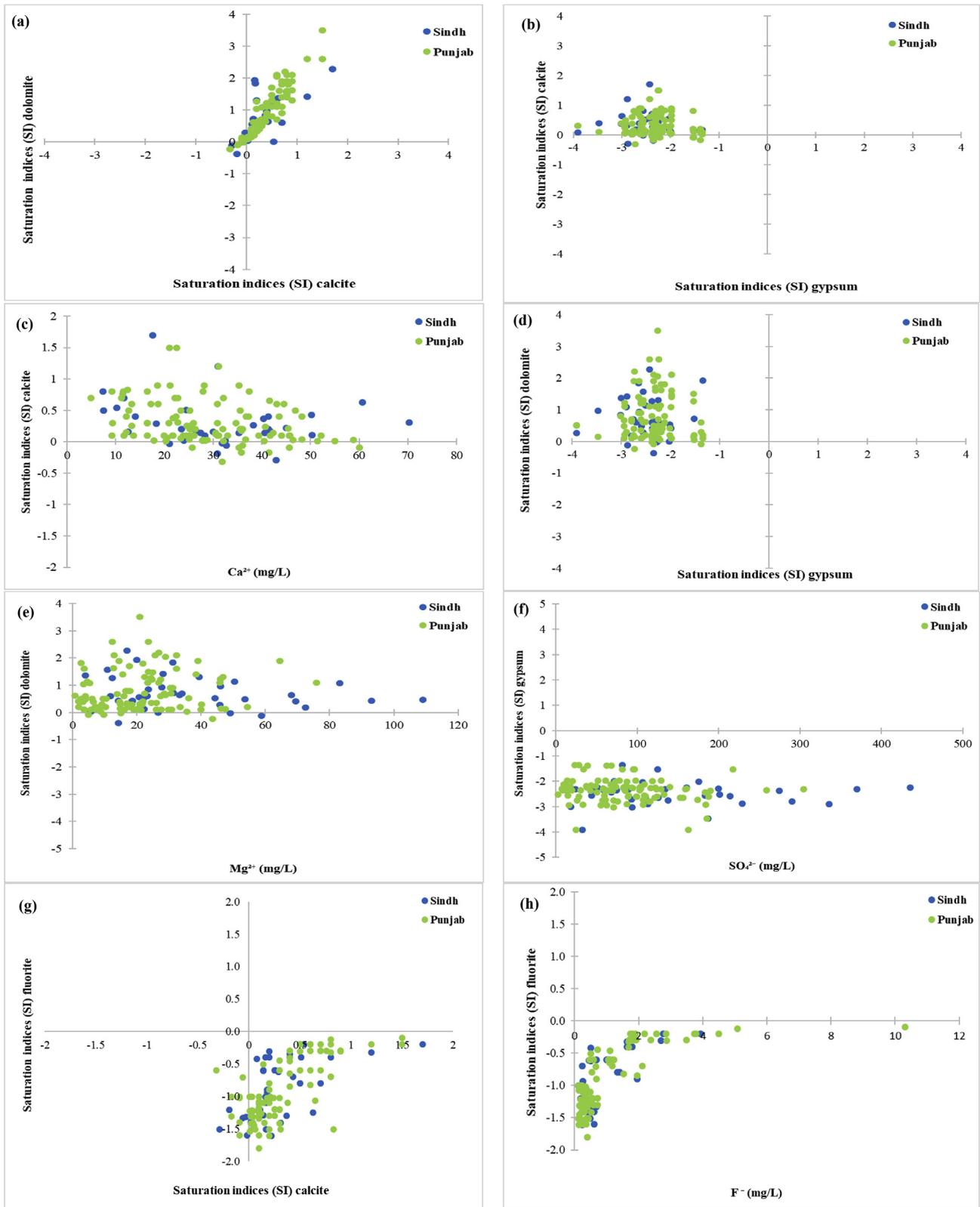


Fig. 9. Saturation indices scattered plots of the study area, dolomite vs calcite (a), calcite vs gypsum (b), calcite versus Ca^{2+} (c), dolomite versus gypsum (d), dolomite versus Mg^{2+} (e), gypsum versus SO_4^{2-} (f), fluorite versus calcite (e) and fluorite versus F^- (f).

cation exchange conditions as well as the anthropogenic activities derived F⁻ concentration in groundwater from the present study area.

The results of present study suggest that most of the groundwater samples along riverine system in Sindh and Punjab contain high F⁻ concentration and consequently residents of these areas are at a high to very high-risk of fluorosis, bone deformation and skeletal fluorosis. Therefore, Government of Pakistan and other environmental authorities should systematically investigate fluorosis cases, and immediately launch rehabilitation measures and F⁻ mitigation program in affected areas. Furthermore, the well testing should be made available at village level along the major rivers to socially mobilize people and assist them switching from F⁻-rich (unsafe) to F⁻-free (safe) groundwater wells. It is also recommended that authorities must employ various water purification techniques such as reverse osmosis (RO) to produce and supply potable water in the affected areas.

This study will be helpful do devise policies regarding F⁻ mitigation in groundwater at both national as well as regional level and for better understanding of the spatial distribution, sources, mobilization and key processes, which drive F⁻ contamination in groundwater along the riverine eco-system specifically in Sindh and Punjab, Pakistan.

Conflicts of interest

The authors declared no conflict of interest.

Acknowledgments

The present work is supported by National Key R&D Program of China (No. 2017YFD0800302) and Natural Science Foundation of China (4157312).

Appendix A. Supplementary data

Supplementary data to this article can be found online at <https://doi.org/10.1016/j.envpol.2019.03.043>.

References

- Alarcón-Herrera, M.T., Bundschuh, J., Nath, B., Nicolli, H.B., Gutierrez, M., Reyes-Gomez, V.M., Nunez, D., Martín-Dominguez, I.R., Sracek, O., 2013. Co-occurrence of arsenic and fluoride in groundwater of semi-arid regions in Latin America: genesis, mobility and remediation. *J. Hazard Mater.* 262, 960–969.
- Ali, W., Mushtaq, N., Javed, T., Zhang, H., Ali, K., Rasool, A., Farooqi, A., 2018a. Vertical mixing with return irrigation water the cause of arsenic enrichment in groundwater of district Larkana Sindh, Pakistan. *Environ. Pollut.* 245, 77–88.
- Ali, W., Rasool, A., Junaid, M., Zhang, H., 2018b. A comprehensive review on current status, mechanism, and possible sources of arsenic contamination in groundwater: a global perspective with prominence of Pakistan scenario. *Environ. Geochem. Health* 1–24.
- APHA, 2005. American Public Health Association. Standard Methods for the Examination of Water and Wastewater, twenty-first ed. American Public Health Association, Washington DC. 1220p.
- Argamasilla, M., Barberá, J., Andreo, B., 2017. Factors controlling groundwater salinization and hydrogeochemical processes in coastal aquifers from southern Spain. *Sci. Total Environ.* 580, 50–68.
- Ayoub, S., Gupta, A.K., 2006. Fluoride in drinking water: a review on the status and stress effects. *Crit. Rev. Environ. Sci. Technol.* 36, 433–487.
- Barzegar, R., Moghaddam, A.A., Tziritis, E., 2017. Hydrogeochemical features of groundwater resources in Tabriz plain, northwest of Iran. *Applied Water Science* 7, 3997–4011.
- Bozdağ, A., 2016. Assessment of the hydrogeochemical characteristics of groundwater in two aquifer systems in Çumra Plain, Central Anatolia. *Environmental earth sciences* 75, 674.
- Brahman, K.D., Kazi, T.G., Afridi, H.I., Naseem, S., Arain, S.S., Ullah, N., 2013. Evaluation of high levels of fluoride, arsenic species and other physicochemical parameters in underground water of two sub districts of Tharparkar, Pakistan: a multivariate study. *Water Res.* 47, 1005–1020.
- Chadha, D., Ray, S., 1999. High Incidence of Arsenic in Groundwater in West Bengal. CGWB, Ministry of Water Resources, Faridabad, India.
- Chanpiwat, P., Sthiannopkao, S., Cho, K.H., Kim, K.-W., San, V., Suvanthong, B., Vongthavady, C., 2011. Contamination by arsenic and other trace elements of tube-well water along the Mekong River in Lao PDR. *Environ. Pollut.* 159, 567–576.
- Dar, M.A., Sankar, K., Dar, I.A., 2011. Fluorine contamination in groundwater: a major challenge. *Environ. Monit. Assess.* 173, 955–968.
- Dehbandi, R., Moore, F., Keshavarzi, B., 2017. Provenance and geochemical behavior of fluorine in the soils of an endemic fluorosis belt, central Iran. *J. Afr. Earth Sci.* 129, 56–71.
- Dupas, R., Gascuel-Oudoux, C., Gilliet, N., Grimaldi, C., Gruau, G., 2015. Distinct export dynamics for dissolved and particulate phosphorus reveal independent transport mechanisms in an arable headwater catchment. *Hydrol. Process.* 29, 3162–3178.
- Edmunds, W.M., Smedley, P.L., 2013. Fluoride in Natural Waters, Essentials of Medical Geology. Springer, pp. 311–336.
- Eqani, S.A.M.A.S., Bhowmik, A.K., Qamar, S., Shah, S.T.A., Sohail, M., Mulla, S.I., Fasola, M., Shen, H., 2016. Mercury contamination in deposited dust and its bioaccumulation patterns throughout Pakistan. *Sci. Total Environ.* 569, 585–593.
- Farooqi, A., Masuda, H., Kusakabe, M., Naseem, M., Firdous, N., 2007. Distribution of highly arsenic and fluoride contaminated groundwater from east Punjab, Pakistan, and the controlling role of anthropogenic pollutants in the natural hydrological cycle. *Geochem. J.* 41, 213–234.
- Gao, X., Wang, Y., Li, Y., Guo, Q., 2007. Enrichment of fluoride in groundwater under the impact of saline water intrusion at the salt lake area of Yuncheng basin, northern China. *Environ. Geol.* 53, 795–803.
- Gibbs, R.J., 1970. Mechanisms controlling world water chemistry. *Science* 170, 1088–1090.
- Islam, M.A., Zahid, A., Rahman, M.M., Rahman, M.S., Islam, M., Akter, Y., Shammi, M., Bodrud-Doza, M., Roy, B., 2017. Investigation of groundwater quality and its suitability for drinking and agricultural use in the south central part of the coastal region in Bangladesh. *Exposure and Health* 9, 27–41.
- Jacks, G., Bhattacharya, P., Chaudhary, V., Singh, K., 2005. Controls on the genesis of some high-fluoride groundwaters in India. *Appl. Geochem.* 20, 221–228.
- Jackson, J.E., 2005. A User's Guide to Principal Components. John Wiley & Sons.
- Jehan, S., Khattak, S.A., Muhammad, S., Ahmad, R., Farooq, M., Khan, S., Khan, A., Ali, L., 2018. Ecological and health risk assessment of heavy metals in the Hattar industrial estate, Pakistan. *Toxin Rev.* 1–10.
- Kaown, D., Koh, D.-C., Mayer, B., Lee, K.-K., 2009. Identification of nitrate and sulfate sources in groundwater using dual stable isotope approaches for an agricultural area with different land use (Chuncheon, mid-eastern Korea). *Agric. Ecosyst. Environ.* 132, 223–231.
- Kelly, W.R., Holm, T.R., Wilson, S.D., Roadcap, G.S., 2005. Arsenic in glacial aquifers: sources and geochemical controls. *Gr. Water* 43, 500–510.
- Khan, S., Rauf, R., Muhammad, S., Qasim, M., Din, I., 2016. Arsenic and heavy metals health risk assessment through drinking water consumption in the Peshawar District, Pakistan. *Hum. Ecol. Risk Assess.* Int. J. 22, 581–596.
- KheradPisheh, Z., Ehrampoush, M., Montazeri, A., Mirzaei, M., Mokhtari, M., Mahvi, A., 2016. Fluoride in drinking water in 31 provinces of Iran. *Exposure and Health* 8, 465–474.
- Kumar, M., Ramanathan, A., Rao, M., Kumar, B., 2006. Identification and evaluation of hydrogeochemical processes in the groundwater environment of Delhi, India. *Environ. Geol.* 50, 1025–1039.
- Li, C., Gao, X., Wang, Y., 2015. Hydrogeochemistry of high-fluoride groundwater at Yuncheng Basin, northern China. *Sci. Total Environ.* 508, 155–165.
- Li, D., Gao, X., Wang, Y., Luo, W., 2018. Diverse mechanisms drive fluoride enrichment in groundwater in two neighboring sites in northern China. *Environ. Pollut.* 237, 430–441.
- Li, P., Qian, H., Wu, J., Chen, J., Zhang, Y., Zhang, H., 2014. Occurrence and hydrogeochemistry of fluoride in alluvial aquifer of Weihe River, China. *Environmental earth sciences* 71, 3133–3145.
- Luo, W., Gao, X., Zhang, X., 2018. Geochemical processes controlling the groundwater chemistry and fluoride contamination in the Yuncheng Basin, China—an area with complex hydrogeochemical conditions. *PLoS One* 13, e0199082.
- Magesh, N., Chandrasekar, N., Elango, L., 2016. Occurrence and distribution of fluoride in the groundwater of the Tamiraparani River basin, South India: a geostatistical modeling approach. *Environmental earth sciences* 75, 1483.
- Moharir, A., Ramteke, D., Moghe, C., Wate, S., Sarin, R., 2002. Surface and groundwater quality assessment in Bina region. *Indian J. Environ. Prot.* 22, 961–969.
- Msonda, K., Masamba, W., Fabiano, E., 2007. A study of fluoride groundwater occurrence in Nathenje, Lilongwe, Malawi. *Phys. Chem. Earth* 32, 1178–1184. Parts A/B/C.
- Mushtaq, N., Younas, A., Mashiatullah, A., Javed, T., Ahmad, A., Farooqi, A., 2018. Hydrogeochemical and isotopic evaluation of groundwater with elevated arsenic in alkaline aquifers in Eastern Punjab, Pakistan. *Chemosphere* 200, 576–586.
- Nakhaei, M., Dadgar, M.A., Amiri, V., 2016. Geochemical processes analysis and evaluation of groundwater quality in Hamadan Province, Western Iran. *Arabian Journal of Geosciences* 9, 384.
- Noli, F., Tsamos, P., 2016. Concentration of heavy metals and trace elements in soils, waters and vegetables and assessment of health risk in the vicinity of a lignite-fired power plant. *Sci. Total Environ.* 563, 377–385.
- Nouri, J., Mahvi, A.H., Babaei, A., Ahmadpour, E., 2006. Regional pattern distribution of groundwater fluoride in the Shush aquifer of Khuzestan County, Iran. *Fluoride* 39, 321.

- Olaka, L.A., Wilke, F.D., Olago, D.O., Odada, E.O., Mulch, A., Musloff, A., 2016. Groundwater fluoride enrichment in an active rift setting: Central Kenya Rift case study. *Sci. Total Environ.* 545, 641–653.
- Podgorski, J.E., Eqani, S.A.M.A.S., Khanam, T., Ullah, R., Shen, H., Berg, M., 2017. Extensive arsenic contamination in high-pH unconfined aquifers in the Indus Valley. *Science advances* 3, e1700935.
- Rafique, T., Naseem, S., Ozsvath, D., Hussain, R., Bhangar, M.I., Usmani, T.H., 2015. Geochemical controls of high fluoride groundwater in Umarkot sub-district, Thar Desert, Pakistan. *Sci. Total Environ.* 530, 271–278.
- Rahmani, A., Rahmani, K., Dobaradaran, S., Mahvi, A.H., Mohamadjani, R., Rahmani, H., 2010. Child dental caries in relation to fluoride and some inorganic constituents in drinking water in Arsanjan, Iran. *Fluoride* 43, 179–186.
- Raj, D., Shaji, E., 2017. Fluoride contamination in groundwater resources of Alleppey, southern India. *Geosci. Front.* 8, 117–124.
- Rashid, A., Guan, D.-X., Farooqi, A., Khan, S., Zahir, S., Jehan, S., Khattak, S.A., Khan, M.S., Khan, R., 2018. Fluoride prevalence in groundwater around a fluorite mining area in the flood plain of the River Swat, Pakistan. *Sci. Total Environ.* 635, 203–215.
- Rashid, A., Khattak, S.A., Ali, L., Zaib, M., Jehan, S., Ayub, M., Ullah, S., 2019. Geochemical profile and source identification of surface and groundwater pollution of District Chitral, Northern Pakistan. *Microchem. J.* 145, 1058–1065.
- Rasool, A., Farooqi, A., Xiao, T., Ali, W., Noor, S., Abiola, O., Ali, S., Nasim, W., 2017. A review of global outlook on fluoride contamination in groundwater with prominence on the Pakistan current situation. *Environ. Geochem. Health* 1–17.
- Rasool, A., Farooqi, A., Xiao, T., Ali, W., Noor, S., Abiola, O., Ali, S., Nasim, W., 2018. A review of global outlook on fluoride contamination in groundwater with prominence on the Pakistan current situation. *Environ. Geochem. Health* 40, 1265–1281.
- Rasool, A., Xiao, T., Baig, Z.T., Masood, S., Mostofa, K.M., Iqbal, M., 2015. Co-occurrence of arsenic and fluoride in the groundwater of Punjab, Pakistan: source discrimination and health risk assessment. *Environ. Sci. Pollut. Control Ser.* 22, 19729–19746.
- Rezaei, M., Nikbakht, M., Shakeri, A., 2017. Geochemistry and sources of fluoride and nitrate contamination of groundwater in Lar area, south Iran. *Environ. Sci. Pollut. Control Ser.* 24, 15471–15487.
- Shahid, M., Niazi, N.K., Dumat, C., Naidu, R., Khalid, S., Rahman, M.M., Bibi, I., 2018. A meta-analysis of the distribution, sources and health risks of arsenic-contaminated groundwater in Pakistan. *Environ. Pollut.* 242, 307–319.
- Sharma, S.K., Subramanian, V., 2008. Hydrochemistry of the Narmada and Tapi rivers, India. *Hydrol. Process.: Int. J.* 22, 3444–3455.
- Sheikhy Narany, T., Ramli, M.F., Aris, A.Z., Sulaiman, W.N.A., Juahir, H., Fakharian, K., 2014. Identification of the hydrogeochemical processes in groundwater using classic integrated geochemical methods and geostatistical techniques. In: Amol-Babol Plain, vol. 2014. The Scientific World Journal, Iran.
- Singaraja, C., Chidambaram, S., Prasanna, M.V., Thivya, C., Thilagavathi, R., 2014. Statistical analysis of the hydrogeochemical evolution of groundwater in hard rock coastal aquifers of Thoothukudi district in Tamil Nadu, India. *Environmental earth sciences* 71, 451–464.
- Soltermann, F., Abegglen, C., Götz, C., Von Gunten, U., 2016. Bromide sources and loads in Swiss surface waters and their relevance for bromate formation during wastewater ozonation. *Environ. Sci. Technol.* 50, 9825–9834.
- Srinivasamoorthy, K., Chidambaram, S., Prasanna, M., Vasanthavihar, M., Peter, J., Anandhan, P., 2008. Identification of major sources controlling groundwater chemistry from a hard rock terrain—a case study from Mettur taluk, Salem district, Tamil Nadu, India. *Journal of Earth System Science* 117, 49.
- Tabassum, R.A., Shahid, M., Dumat, C., Niazi, N.K., Khalid, S., Shah, N.S., Imran, M., Khalid, S., 2018. Health risk assessment of drinking arsenic-containing groundwater in Hasilpur, Pakistan: effect of sampling area, depth, and source. *Environ. Sci. Pollut. Control Ser.* 1–12.
- Taheri, M., Gharaie, M.H.M., Mehrzad, J., Afshari, R., Datta, S., 2017. Hydrogeochemical and isotopic evaluation of arsenic contaminated waters in an argillic alteration zone. *J. Geochem. Explor.* 175, 1–10.
- Tahir, M., Rasheed, H., 2013. Fluoride in the drinking water of Pakistan and the possible risk of crippling fluorosis. *Drink. Water Eng. Sci.* 6, 17–23.
- Tirkey, P., Bhattacharya, T., Chakraborty, S., Baraik, S., 2017. Assessment of Groundwater Quality and Associated Health Risks: a Case Study of Ranchi City, Jharkhand, India, vol. 5. Groundwater for Sustainable Development, pp. 85–100.
- Van Wirdum, G., 1980. Description of water-quality changes in a hydrological cycle, for the purpose of nature conservation. Waterquality in groundwater-flow systems. In: Hooghart, J.C. (Ed.), Commission for Hydrological Research TNO, vol. 5, pp. 118–143. The Hague, The Netherlands, Reports and notes.
- Vázquez-Guerrero, A., Alfaro-Cuevas-Villanueva, R., Rutiaga-Quiñones, J.G., Cortés-Martínez, R., 2016. Fluoride removal by aluminum-modified pine sawdust: effect of competitive ions. *Ecol. Eng.* 94, 365–379.
- Vithanage, M., Rajapaksha, A.U., Bootharaju, M., Pradeep, T., 2014. Surface complexation of fluoride at the activated nano-gibbsite water interface. *Colloid. Surf. Physicochem. Eng. Asp.* 462, 124–130.
- Wilcox, L.V., 1958. Water quality from the standpoint of irrigation. *Journal (American Water Works Association)* 50, 650–654.
- Zabala, M., Manzano, M., Vives, L., 2016. Assessment of processes controlling the regional distribution of fluoride and arsenic in groundwater of the Pampeano Aquifer in the Del Azul Creek basin (Argentina). *J. Hydrol.* 541, 1067–1087.